Infrared Multiphoton Dissociation (IRMPD) and Collisionally Activated Dissociation of Peptides in a Quadrupole Ion Trap with Selective IRMPD of Phosphopeptides

Matthew C. Crowe and Jennifer S. Brodbelt
Department of Chemistry and Biochemistry, The University of Texas at Austin, Austin, Texas, USA

Dissociation of protonated peptides via infrared multiphoton dissociation (IRMPD) provides more extensive sequence information than is obtained with collisionally activated dissociation (CAD) in a quadrupole ion trap due to the lack of the CAD low *m/z* cutoff and the ability to form secondary and higher order fragments with the non-resonant photoactivation technique. In addition, IRMPD is shown to be useful for the selective dissociation of phosphopeptides over those which are not phosphorylated because the greater photon absorption efficiency of the phosphorylated peptides leads to their more rapid dissociation. Finally, the selectivity of the IRMPD technique for phosphorylated species in complex mixtures is confirmed with the analysis of a mock peptide mixture and a tryptic digest of α-casein. (J Am Soc Mass Spectrom 2004, 15, 1581–1592) © 2004 American Society for Mass Spectrometry

Investigations into the protein complement of an organism's genome seek to identify the primary structure of the proteins produced including any modifications that take place. Following transcription, the primary sequence of a protein can undergo modifications such as N-terminal acetylation, formation of disulfide bonds, sulfation, and phosphorylation, all of which affect activity. Arguably, the most important post-translational modification of proteins is the reversible phosphorylation of serine, threonine, and tyrosine residues [1, 2]. This covalent modification has regulatory influence over cellular processes such as metabolism, growth, and reproduction [3–5]. Because phosphorylation has such an impact on living systems, it is of great interest to be able to determine when, where, and to what extent this type of modification takes place. For this, suitable analytical techniques must be developed and applied. The relative speed and sensitivity of tandem mass spectrometry make it a powerful tool [6–30] when compared with more conventional methods of phosphoprotein mapping, namely ^{32}P phosphate labeling of a protein sample followed by purification, enzymatic digestion, chromatographic separation, and Edman sequencing.

Collisional activated dissociation (CAD) typically reveals sites of phosphorylation based on a mass loss associated with the cleavage of a phosphate moiety from a peptide ion (-80 (HPO_3) and/or -98 (H_3PO_4) in positive ion MS/MS) [9, 14]. Precursor ion scanning [14, 19], neutral loss scanning [23], and nozzle-skimmer dissociation [9] can determine the presence, absence, and location of peptide phosphorylation based on the unique mass losses associated with phosphorylated peptides. In MALDI-TOF mass spectrometry, post-source decay (PSD) of metastable ions formed in the source region via these characteristic pathways can also be used to determine sites of phosphorylation [17]. When a peptide is phosphorylated at a tyrosine residue as opposed to a serine or threonine residue, however, the unique neutral losses are not necessarily observed upon dissociation due to the greater phosphate-tyrosine binding energy and the existence of fewer β-elimination pathways than are present in the cases of serine and threonine phosphorylation [10, 22]. As a result, the techniques that rely on a common neutral loss from all phosphorylated peptides are often not reliable for tyrosine-phosphorylated species. Some of the limitations of these tandem mass spectrometry techniques for the determination of phosphorylation sites can be overcome in FTICR analyzers with the use of electron capture dissociation (ECD) [31–37], which allows fragmentation of peptides without the loss of the phosphate group [21, 24, 29–31]. This technique provides valuable and extensive sequence information in the form of fragment ions complementary to those produced with CAD or IRMPD, though often at lower relative abundances. Electron capture dissociation is unfortunately difficult to implement on a quadrupole ion trap, and the promising electron transfer dissociation experiments recently pioneered by Syka et al. [38] on a linear ion trap

Published online September 18, 2004
Address reprint requests to Dr. J. S. Brodbelt, Department of Chemistry and Biochemistry, University of Texas at Austin, 1 University Station A5300, Austin, TX 78712-0165, USA. E-mail: jbrodbelt@mail.utexas.edu

1044-0305/04/$30.00
doi:10.1016/j.jasms.2004.07.016

Received April 28, 2004
Revised July 23, 2004
Accepted July 26, 2004

require multiple ionization sources, relatively complex scan functions (necessary for simultaneous trapping of positive and negative ions followed by reaction of these species), and results in fragment ions of lower abundances when compared with those obtained by CAD and IRMPD.

Infrared multiphoton dissociation, which has proven to be a viable alternative to collisional activation in trapping mass spectrometers, can also be used to circumvent some of the problems encountered with activation techniques that rely on common neutral losses for the detection of phosphopeptides and is relatively easy to implement [22, 25, 27, 28, 30, 35, 39–60]. Because of the suitably low background pressures used in FTICR mass spectrometry, IRMPD has been applied extensively with much success [22, 25, 27, 28, 30, 35, 39–47]. Additionally, Hofstadler et al. have had considerable success applying IRMPD to a hexapole ion trap (external to an FTICR analyzer) for characterization of oligonucleotide molecules [46]. Although less common than in FTICR instruments, several groups have also explored IRMPD in the quadrupole ion trap [48–60]. IRMPD in a quadrupole ion trap has several inherent advantages over the more conventional CAD technique (as well as over electron-transfer dissociation, as previously discussed). IRMPD is more efficient in some cases than CAD for MS^n experiments since IRMPD requires no alteration of the stable trajectory or kinetic energy of the trapped ions for excitation, as is necessary for CAD. This reduces the extent of ion loss through scattering relative to collisional activation. In addition, the low *m/z* cutoff (approximately one third of the *m/z* value of the precursor ion) necessary for efficient CAD is not required in IRMPD experiments, increasing the effective *m/z* range of the ion trap instrument for the analysis of fragment ions [55]. This loss of the lower one third of the *m/z* range in CAD experiments is related to the level of the rf voltage needed to provide an adequate activation environment for the precursor ions at the expense of storage of the lower *m/z* ions. The non-resonant IRMPD technique results in formation of secondary and higher order fragments which can provide additional structural information to that obtained in a single resonant collisional activation experiment.

We have found the IRMPD technique to be well suited for the sequencing of peptide molecules, in particular those which are phosphorylated. In the present study, we apply IRMPD to a wide variety of peptides to determine its analytical utility relative to collisional activation in a quadrupole ion trap. We have focused on phosphorylated peptides because of the importance of phosphorylation in biological systems and the unique absorption properties of the phosphate group which make it a powerful chromophore for 10.6 μm light (the wavelength generated by the CO_2 lasers used in these experiments), resulting in selective dissociation of phosphorylated peptides [39, 61]. Flora and Muddiman have shown notable results using IRMPD in an FTICR instrument to selectively dissociate phosphorylated peptide ions in mixtures, as well as to investigate the activation energies, dissociation rate constants, and absorption properties of phosphorylated peptides [22, 25, 28]. Muddiman's group has reported IRMPD results for negatively-charged phosphorylated peptides [22, 25, 28], while the present study evaluates positively charged ions. The results presented here demonstrate the potential applicability of IRMPD for de novo sequencing and sequence tag generation for protein identification; particularly for investigations in phosphoproteomics.

Experimental

Collisionally activated dissociation (CAD) experiments were performed on a Finnigan LCQ-Duo ion trap mass spectrometer with an electrospray source using the Xcalibur (Finnigan, San Jose, CA) software package. The pressure was maintained at nominally 5×10^{-6} torr with helium in the absence of sample introduction. Solutions of 1–10 μM analyte (0–20% H_2O in MeOH) were infused by a syringe pump (Harvard Apparatus, Holliston, MA) at a flow rate of 3 μL/min. During ESI experiments the pressure in the analyzer region increased to nominally 1×10^{-5} torr and remained constant throughout all experiments. Ionization and trapping conditions were optimized for each solution analyzed. Conceivably the rate of sample consumption could be reduced by several orders of magnitude by equipping the mass spectrometer with a nanospray source; this would make the methods described herein applicable to smaller scale biological samples.

Infrared multiphoton dissociation (IRMPD) experiments were performed on two ion trap mass spectrometers, each equipped with homebuilt ESI sources. Two IRMPD instruments were employed in the present work to demonstrate both the versatility of the IRMPD technique and its applicability to home-built as well as commercial systems. The first instrument was a quadrupole ion trap system built in-house that used modified ITD electronics and ICMS software (University of Florida, Gainesville, FL) with an ESI source and interface modeled after the Oak Ridge National Laboratory design [62]. Details of this instrument have been presented previously [49]. Analyzed solutions were prepared in 100% methanol. Concentrations and sample introduction were unchanged from above. The pressure in the ion trap region of the instrument during ESI was nominally 9.5×10^{-5} torr for all experiments. A stored waveform inverse Fourier transform (SWIFT) system controlled by TTL triggers in the scan function was used for resonant ejection and has been described in detail previously [49]. IRMPD experiments were performed with either an Apollo 50 W continuous-wave CO_2 laser (Model 575, Apollo Lasers, Chatsworth, CA) with a Uniblitz shutter (Vincent Associates, Rochester, NY), or a Synrad 50 W continuous-wave CO_2 laser (Series 48, Model 48-5, Synrad, Mukilteo, WA). Both the Apollo shutter and the Synrad output were controlled

by TTL triggers in the scan function, allowing control of the irradiation time. The trapping volume was irradiated through a ZnSe window in the vacuum chamber aligned with a 6 mm hole drilled radially in the ring electrode [49]. IRMPD laser irradiation time was varied between 2 and 1000 ms as needed at a flux of 45 W/cm^2.

The second instrument used for IRMPD was a modified M-8000 Hitachi 3DQ ion trap mass spectrometer using the 3DQ software package and a homebuilt ESI source. The pressure in the analyzer vacuum chamber was nominally 5.1×10^{-5} torr unless otherwise specified. Solutions of 10–50 μM analyte (0–20% H_2O in MeOH) were infused by a syringe pump at a flow rate of 3 μL/min. IRMPD experiments on this instrument were performed with the previously mentioned Synrad CO_2 laser, with gating controlled by software TTL triggers. The trapping volume was irradiated through a ZnSe window in the vacuum chamber aligned with a 4 mm hole in the ring electrode. On this instrument, the irradiation time was kept constant (t = 50 ms) while the background gas pressure and laser power were adjusted to regulate IRMPD efficiency and extent of fragmentation. CAD data was also acquired on this instrument for direct comparison with the IRMPD data.

The laser power used for these experiments is high compared with those used for IRMPD in FTICR analyzers because of the collisional deactivation that occurs upon interactions with analyte ions and bath gas molecules in a quadrupole ion trap; collisional deactivation does not occur to an appreciable extent at the reduced pressure of an ICR cell. In addition, in these experiments, the beam is unfocussed (diameter = 4.0 mm) so that it easily encompasses the ion trapped ion volume (diameter = ~1.0 mm); the fact that the beam is unfocussed also increases the power necessary to induce dissociation.

Model peptides were obtained from Sigma Chemical (St. Louis, MO) (angiotensin I, bradykinin, bradykinin fragment 1–8, bradykinin fragment 2–9, γ-endorphin, melittin), BACHEM (King of Prussia, PA) (Val^5-angiotensin I, Val^5, Asn^9-angiotensin I, tyr-bradykinin, lys-bradykinin), and AnaSpec (San Jose, CA) (angiotensin II). Modified peptides (phosphorylated angiotensin II substrate, phosphorylated kinase domain of insulin receptor, triply phosphorylated kinase domain of insulin receptor, tyrosine protein kinase substrate JAK 2, phosphorylated protein kinase substrate-2, PKA inhibitor substrate) were obtained from AnaSpec. α-casein was obtained from Sigma Chemical (St. Louis, MO).

Casein was enzymatically digested with immobilized TPCK trypsin (Pierce, Rockford, IL) in 50 mM ammonium bicarbonate buffer (pH = 8.0) for 16 h at 37° C. The product was then centrifuged to separate the immobilized trypsin beads from the digested protein solution. The supernatant was removed and diluted to the desired concentration (10 μM) in 50:50 H_2O:methanol. Acetic acid (~1%) was added to the solution to promote peptide protonation.

Results and Discussion

IRMPD versus CAD of Model Peptides

To compare the utility of IRMPD and CAD for sequencing peptides in a quadrupole ion trap, the tandem mass spectrometry results obtained for several model peptides are presented. Bradykinin and melittin have been examined extensively by other groups, so these peptides are suitable for an initial assessment of IRMPD. The comparison of results obtained for the dissociation of doubly protonated bradykinin using IRMPD and CAD is illustrated in Figure 1. Aside from the additional information obtained in the IRMPD experiment below *m/z* 130 (the low *m/z* cutoff in the CAD experiment), the sequence information obtained from the two experiments is similar. In both cases, sequence coverage is extensive and the relative abundances of the fragment ions in both experiments are alike. There are, however, abundant ions observed in the low *m/z* region of the IRMPD spectrum that are absent in the CAD spectrum, including several corresponding to individual amino acid residues. These ions are potentially useful for sequencing, particularly for assessing covalent post-translational modifications, such as the alkylation of arginine residues. Analogous results are observed for all of the peptides studied (results not shown).

To further assess the utility of IRMPD, the photoactivation results obtained with a significantly larger peptide, melittin (2845.7 Da), are compared to those obtained with CAD. The dissociation results for the $[M + 4H]^{4+}$ precursor ion are shown in Figure 2. The most abundant fragment ions (y_{13}^{3+}, y_{13}^{2+}, y_{24}^{2+}, y_{15}^{2+}, y_{17}^{2+}, b_{12}^{+}, and b_{13}^{+}) are observed in both spectra. More extensive sequence information however, is obtained with IRMPD than CAD. Some of these important sequence ions fall below the low *m/z* cutoff in the CAD experiment in the form of internal fragment ions (PA, PA-28, LT-H_2O) and single amino acid ions (K, P). Other unique ions (y_5^{3+}, y_4^{2+}, b_8^{2+}, y_8^{3+}, b_6^{+}, y_9^{2+}, y_{10}^{2+}, etc.) are also present due to higher order fragmentation, a process which does not occur to a significant extent with CAD.

For triply protonated melittin (data not shown), the sequence ions produced from IRMPD also offer more sequence information than obtained with CAD, again including numerous low *m/z* ions that are absent from the CAD mass spectrum. Three C-terminal (y_2^{+}, y_3^{2+}, y_4^{2+}, y_4^{3+}) and two N-terminal (a_3^{+}, b_3^{+}) sequence ions are observed that are unique to the IRMPD data. In addition to the fragment ions gained in the low *m/z* region of the IRMPD spectrum, there are a considerable number of additional sequence ions which are absent in the CAD spectrum (b_{24}^{2+}, y_8^{+}, b_{12}^{+}, y_7^{+}, b_{10}^{+}, y_{25}^{3+}, y_{23}^{3+}, y_{22}^{3+}, b_{23}^{3+}, b_{12}^{2+}, y_{10}^{3+}, y_3^{+}, y_6^{2+}, y_9^{3+}, y_8^{3+}, y_7^{3+}). These additional fragments most likely result from higher order fragmentation in the IRMPD experiment; these processes

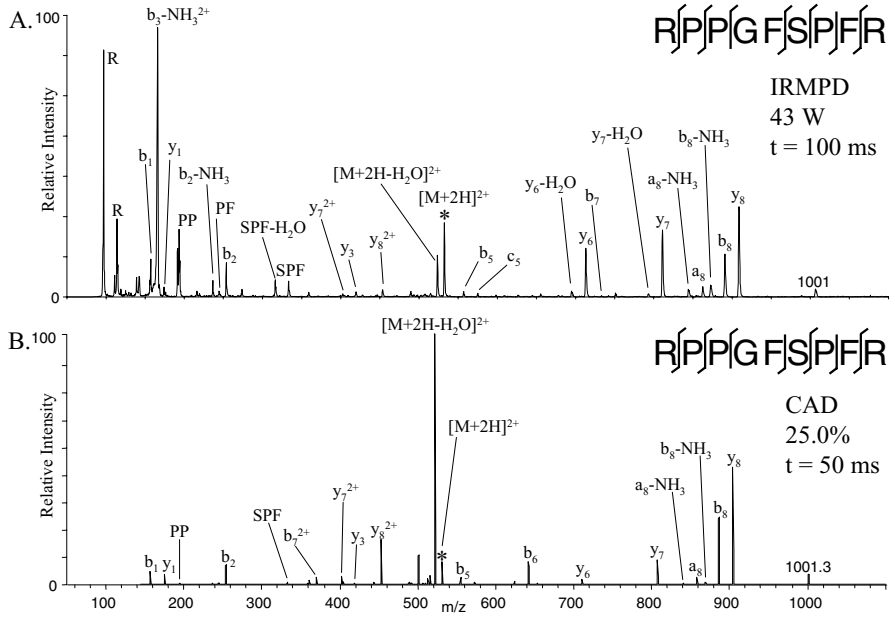

Figure 1. IRMPD versus CAD mass spectra of doubly protonated bradykinin (RPPGFSPFR). The precursor ions are indicated by asterisks.

occur to a lesser extent with collisional activation because it is selective for a particular precursor.

These results demonstrate that the dissociation efficiency of IRMPD in a quadrupole ion trap is sufficiently high to produce extensive fragmentation of peptides. In addition, the spectra presented show IRMPD to have several advantages over collisional activation for peptide characterization. The lack of a low-*m/z* cutoff in IRMPD, an obstacle in CAD experiments, allows for ions at the low end of the *m/z* range to be trapped and analyzed, giving more complete sequence information. In the mid to upper *m/z* range,

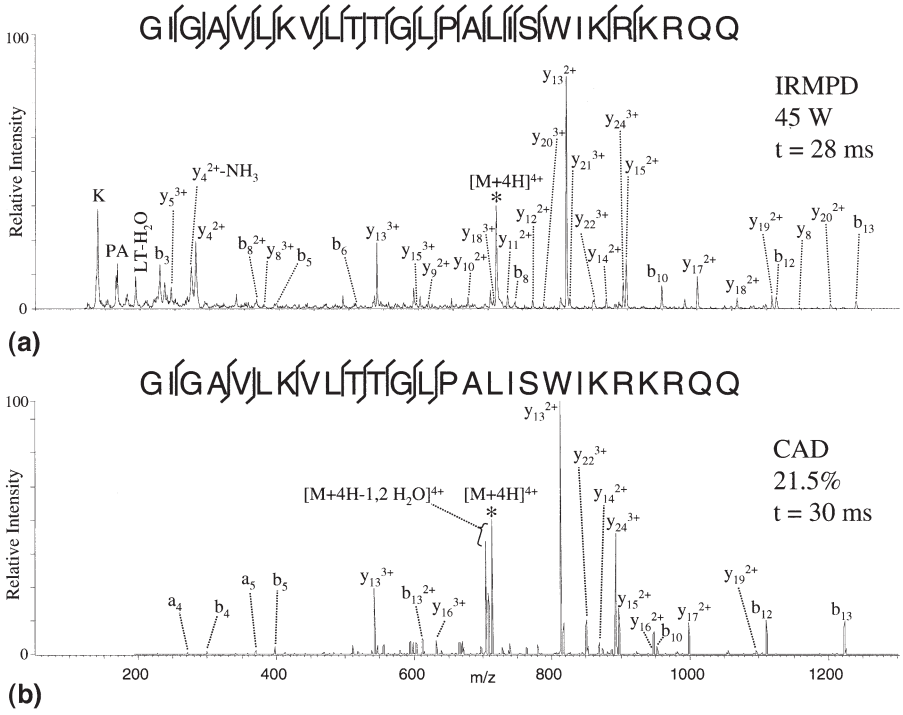

Figure 2. (**a**) IRMPD and (**b**) CAD mass spectra of the $[M + 4H]^{4+}$ melittin precursor ion. The precursor ions are indicated by asterisks.

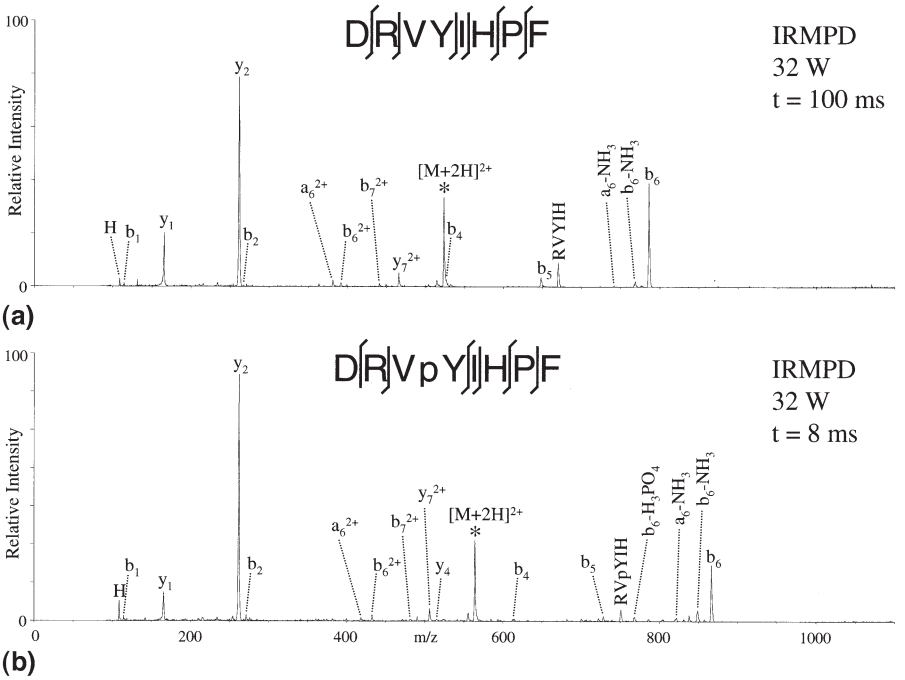

Figure 3. IRMPD mass spectra of (**a**) doubly protonated angiotensin II and (**b**) doubly protonated phosphorylated angiotensin II. The precursor ions are indicated by asterisks.

the fragment information obtained with these two techniques is similar although some sequence information is gained from higher order fragmentation with IRMPD.

IRMPD and CAD of Modified Peptides

IRMPD is also useful for the structural characterization of phosphorylated peptides. The phosphorylated functional groups are strong chromophores due to the efficient absorption of 10.6 μm light by P–O bonds [61]. Several experiments demonstrate that IRMPD in a quadrupole ion trap is markedly more efficient for phosphorylated peptides than it is for those that are not phosphorylated. To systematically demonstrate the dissociation efficiency of IRMPD for phosphorylated and unphosphorylated peptides, the IRMPD results obtained for angiotensin II and tyrosine-phosphorylated angiotensin II, analyzed individually as well as simultaneously, are presented. Figure 3 shows the IRMPD results for doubly protonated angiotensin II and phosphorylated angiotensin II as well as a comparison of the irradiation time necessary to produce comparable extents of dissociation. Similar dissociation patterns are observed for both species, but more than an order of magnitude greater irradiation time is necessary to produce a similar degree of dissociation for the unphosphorylated peptide. In simultaneous analysis of the two angiotensin II peptides, the doubly protonated species are isolated (Figure 4a) and then irradiated. At short irradiation times, (Figure 4b, t = 3 ms), only the phosphorylated precursor dissociates. When the irradiation time is increased substantially (Figure 4c, t = 92 ms), the unphosphorylated precursor dissociates as well, producing fragment ions characteristic of this peptide. The peak at *m/z* 263 corresponds to the y_2^+ ion formed from both precursor ions, accounting for its increase in intensity from Figure 4b to c. To confirm that the phosphorylated peptide does not have an intrinsically lower dissociation energy, energy-variable CAD experiments were undertaken for each peptide. The CAD voltages required to convert 10% of the precursor ions to fragment ions are 19.1 $\pm$ 0.4% and 18.8 $\pm$ 0.4% for angiotensin II and phosphorylated angiotensin II, respectively. This illustrates that the energy required for dissociation does not vary significantly with the presence or absence of a phosphate group and offers further confirmation that the high dissociation efficiency of the phosphorylated peptide is due to its greater IR absorptivity, not a lower energy threshold.

To further demonstrate the ability of IRMPD to provide sequence information, the fragmentation results obtained for a series of larger phospho-peptides (singly phosphorylated Kinase Domain of Insulin Receptor (p-KDIR), triply phosphorylated KDIR (p^3-KDIR), and Tyrosine Kinase Receptor JAK 2) with IRMPD and CAD on the modified Hitachi 3DQ system are presented. In the spectra obtained for p-KDIR (Figure 5), similar fragments are present in each spectrum, with the loss of H_3PO_4 being the dominant fragmentation pathway in both cases. The diagnostic sequence ions have greater abundances in the IRMPD spectrum, although most are present to some extent in both spectra with the exception of two important low

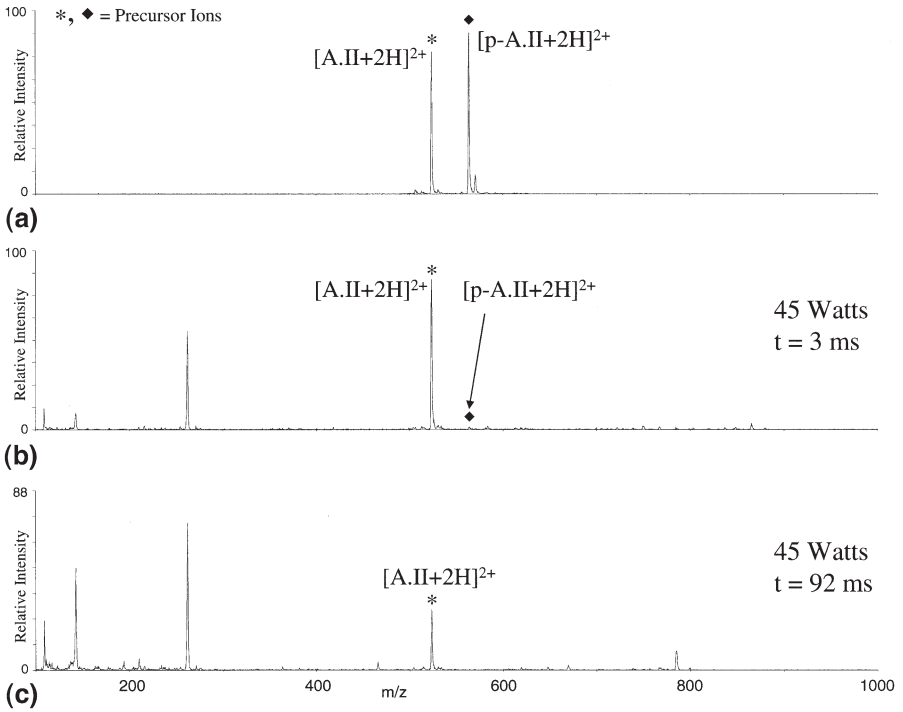

Figure 4. (**a**) Isolation of doubly protonated precursor ions of angiotensin II and phosphorylated angiotensin II, (**b**) IRMPD t = 3ms, (**c**) IRMPD t = 92 ms.

m/z sequence ions, b_2^+ and y_1^+, which are only present in the IRMPD spectrum. Due to the low *m/z* fragments and the greater intensity of useful sequence fragments in the rest of the spectrum, more sequence information is obtained from the IRMPD spectrum.

Analysis of the triply phosphorylated KDIR peptide

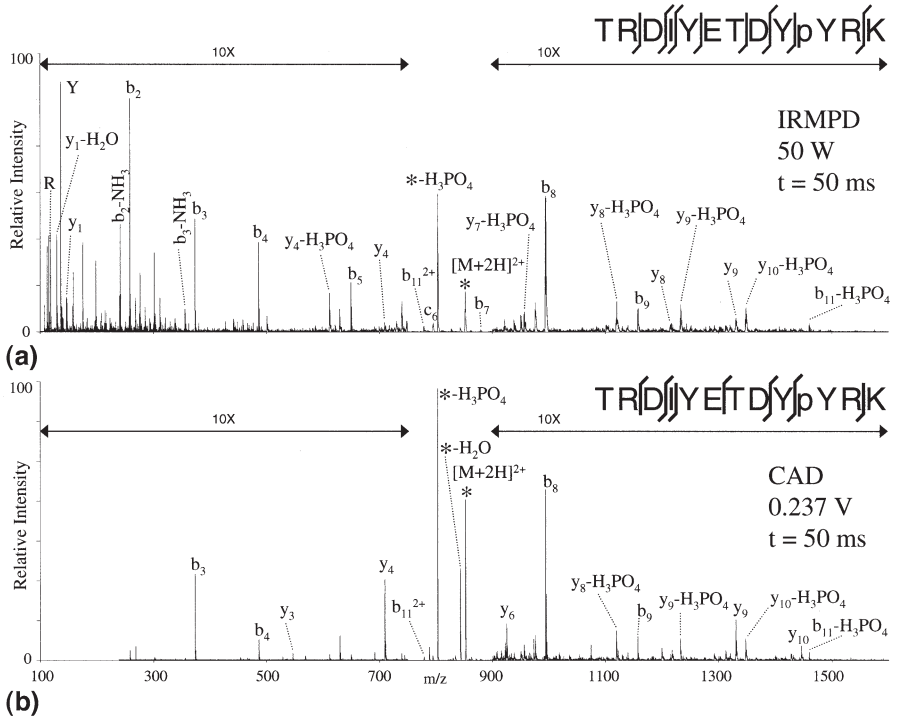

Figure 5. (**a**) IRMPD and (**b**) CAD mass spectra of doubly protonated, singly phosphorylated KDIR. The precursor ions are indicated by asterisks.

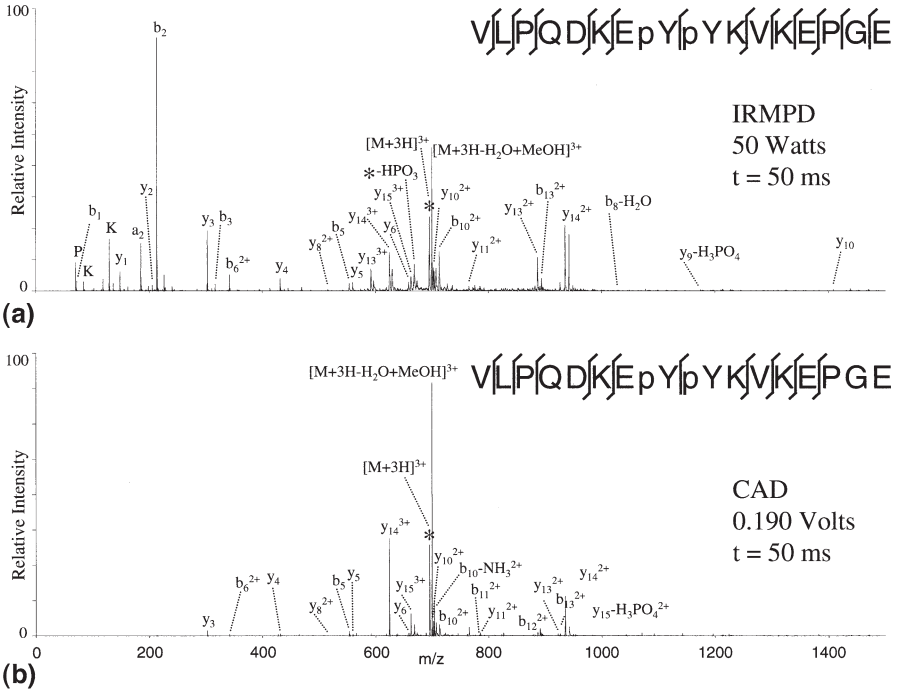

Figure 6. (**a**) IRMPD and (**b**) CAD mass spectra of triply protonated tyrosine kinase receptor JAK 2. The precursor ions are indicated by asterisks.

(data not shown) yields similar results to the singly phosphorylated peptide in terms of relative sequence coverage acquired with CAD and IRMPD. The fragments obtained using both techniques are comparable with the IRMPD technique providing more low *m/z* fragment information (i.e., the terminal b_1^+ and y_1^+ ions are only present in the IRMPD spectrum). Comparison of the IRMPD mass spectra of the triply protonated KDIR peptides (both mono- and tri-phosphorylated) reveals that, even when exposed to considerably lower laser power (at equal irradiation times), the triply phosphorylated KDIR dissociates far more efficiently than the singly phosphorylated species. This data, along with that presented in Figures 3 and 4, provides additional evidence that the presence of a phosphate group increases the efficiency of photodissociation with 10.6 μm light. This trend has been carefully studied by the Muddiman group as well, based on dissociation kinetics in an FTICR instrument [25, 28].

To further demonstrate the effectiveness of photoactivation for sequencing phosphorylated peptides, the IRMPD results obtained for Tyrosine Kinase Receptor JAK 2 peptide (2080.9 Da) are also presented. The results of the dissociation of the triply protonated peptide using both activation techniques are shown in Figure 6. The IRMPD results provide good sequence coverage, including sequence information in the low *m/z* region for the b_{1-3}^+ and y_{1-2}^+ fragments which are absent in the CAD spectrum and provide valuable sequence information.

The peptides mentioned thus far are phosphorylated at tyrosine residues which typically produce more sequence information upon activation than do peptides phosphorylated at serine and threonine residues [10, 22]. To assess the effectiveness of IRMPD for the dissociation of other phosphorylated peptide species, the results obtained for serine phosphorylated (GRT-GRRNpSIHDIL) and threonine phosphorylated (KRpTIRR) peptides are evaluated. Typically, peptides that are phosphorylated at serine and threonine residues do not fragment along the peptide backbone to produce useful sequence ions but instead preferentially lose the phosphate group as H_3PO_4 or HPO_3 [10]. These losses imply the presence of a phosphorylation site, but give no information about the specific location of the phosphate group. Secondary fragmentation information based on subsequent dissociation of the de-phosphorylated product ions however, can be valuable in sequencing these peptides, particularly if a peptide has only one potential phosphorylation site (S, Y, or T) present. The main drawback of undertaking MS^n experiments via CAD is that it involves two or more resonant activation steps, each of which requires tuning for the precursor ion of interest and results in some ion loss due to scattering. With IRMPD, not only is primary fragmentation observed but, depending on the length of time that the fragment ions are irradiated, secondary and higher order fragment information can be obtained in a single experiment, all with minimal ion scattering.

A comparison of the sequence information obtained for a pair of serine/threonine phosphorylated peptides using IRMPD (with short and extended irradiation times) and multi-step CAD is presented to demonstrate the effectiveness of the photoactivation technique for

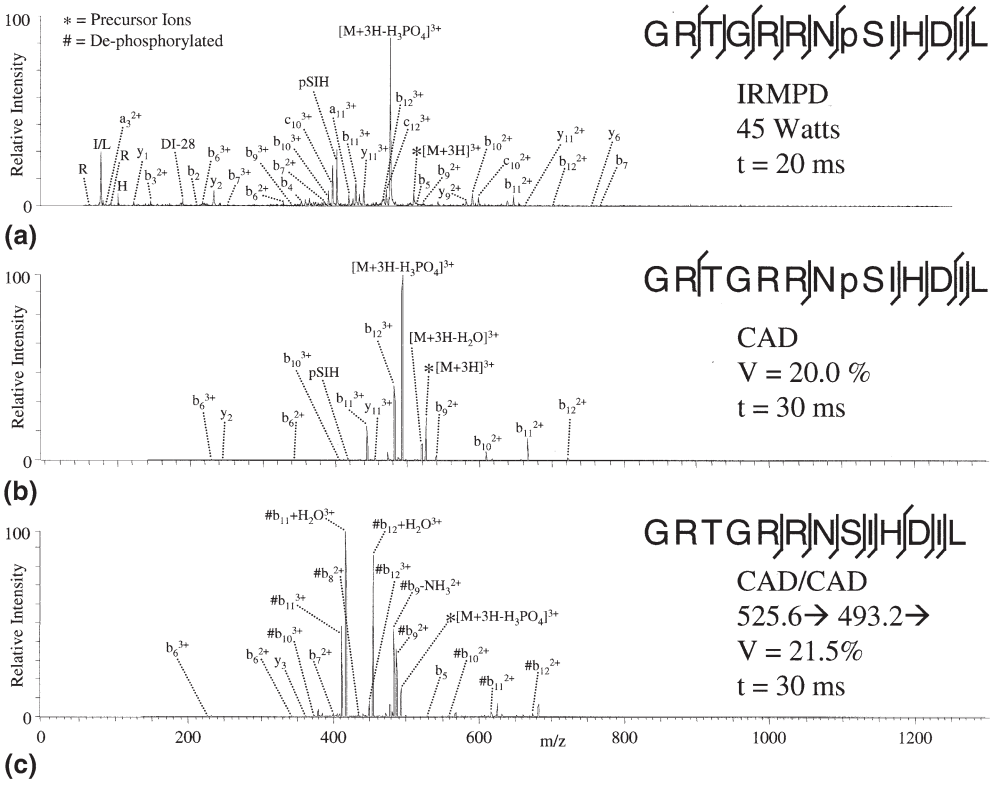

Figure 7. (**a**) IRMPD, (**b**) CAD MS^2, and (**c**) CAD MS^3 mass spectra of triply protonated GRTGRRNpSIHDIL.

the analysis of these types of peptides. The IRMPD and CAD results obtained for the triply protonated peptide, serine-phosphorylated peptide GRTGRRNpSIHDIL (1573.8 Da), are shown in Figure 7. The major fragmentation pathway is the loss of H_3PO_4, which limits the amount of sequence information obtained in the CAD experiment (Figure 7b). A second CAD step (Figure 7c) yields additional structural information in the form of previously absent b-ions (b_5^+, b_7^+, b_8^+), producing an eight-residue sequence tag when information from both the MS^2 and MS^3 spectra are considered. As apparent when the spectra in Figure 7 are compared, the sequence information obtained with a single IRMPD irradiation step (t = 20 ms, Figure 7a) is considerably greater than that obtained with two sequential CAD steps due to the higher order fragmentation pathways promoted by IRMPD and the inability to trap low *m/z* ions in the CAD experiment.

To further demonstrate the usefulness of the IRMPD technique for sequencing peptides phosphorylated at aliphatic residues, the results of an analogous experiment performed with a threonine-phosphorylated peptide, KRpTIRR, are described. In both the IRMPD and CAD experiments, the dominant fragmentation pathway is the loss of H_3PO_4 (data not shown). In addition to the abundant fragment ion due to the loss of 98 Da, a series of low abundance ions are present corresponding to informative b and y sequence ions. By extending the irradiation time in the IRMPD experiment, further primary and secondary fragmentation becomes evident. Full sequence coverage is obtained, and all possible b and y ions are present. A second stage of CAD fails to produce as extensive sequence information, mostly because a single fragmentation channel is dominant in the MS^3 experiment as well as in MS^2. Only two abundant ions are observed: one as a result of loss of water from the precursor, and the other from the loss of a portion of an arginine guanidinium side chain. Both of these losses are facile and produce little or no useful sequence information. Because IRMPD promotes primary, secondary, and further fragmentation, even when uninformative dissociation pathways are the most energetically favorable (as is the case for KRpTIRR), extensive sequence information can still be obtained.

Selective Phosphopeptide Dissociation

To demonstrate the utility of the elevated 10.6 μm-absorption of phosphorylated peptides, the spectra obtained from an IRMPD experiment conducted on a nine-peptide mixture are presented. A mass spectrum obtained from a solution containing ~10 μM of the peptides GGK, AAAAR, YGGFL, bradykinin fragment 1-8, KRpTIRR, angiotensin II, phosphorylated angiotensin II, GRTGRRNpSIHDIL, and Val^5-angiotensin I in 98% methanol/1% acetic acid is shown in Figure 8a. The mass spectral peaks vary in intensity due to the different spray efficiencies of the peptides and slight

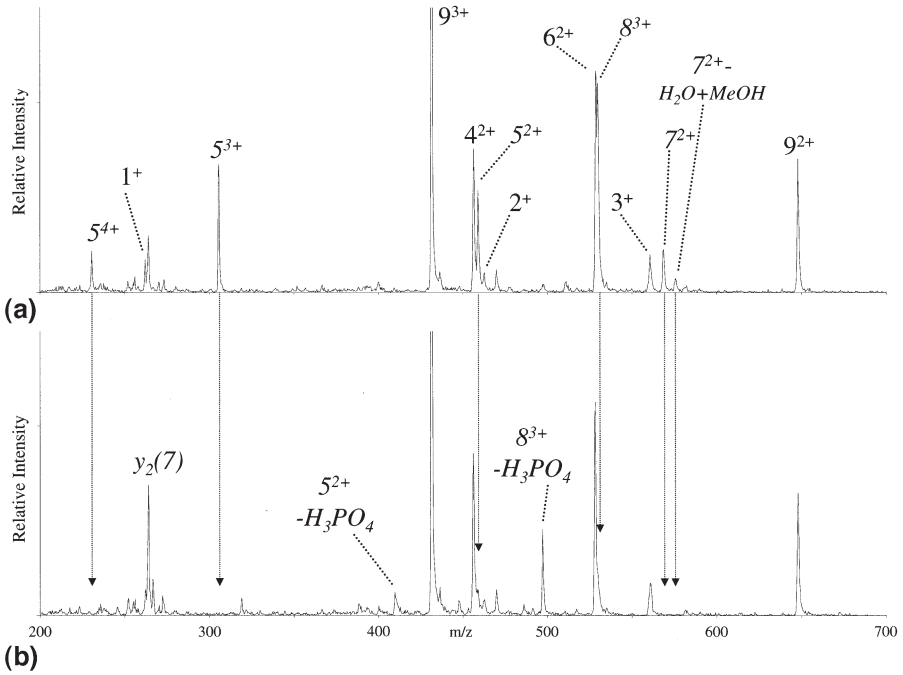

Figure 8. IRMPD mass spectra of mock mixture (**a**) t = 0 ms, (**b**) t = 15 ms (45 watts).

variations in peptide concentrations in the solution. The results observed when the spectrum is examined at 0 ms (Figure 8a) and 16 ms irradiation time (Figure 8b) are striking. The abundances of the unphosphorylated ions in the spectra are unaffected after short irradiation times while the phosphorylated species are completely dissociated. In fact, the non-phosphorylated ions do not undergo notable dissociation until after 180 ms of IR irradiation (data not shown), indicating that, with IRMPD, there is considerable capacity to differentiate the phosphorylation state of peptides.

The capability to selectively dissociate phosphorylated compounds in a mixture also has important implications for the analysis of tryptic digests of phosphorylated proteins. Screening a digest mixture for phosphorylated components in a single ESI-IRMPD-MS experiment could be used as an assay to determine the phosphorylation state of the components in the digest, eliminating the need to extensively analyze every ion in the mass spectrum. To demonstrate the feasibility of this assay, the analysis of a tryptic digest of α-casein with and without IR irradiation is presented. The results of ESI-MS analysis of the tryptic digest dissolved in a 49/49/2 water/methanol/acetic acid are shown in Figure 9a. Peaks are present in the mass spectrum representing the vast majority of the expected tryptic fragments. Alpha-casein is phosphorylated on six residues, ^{79}S, $^{81-83}$S, ^{90}S, and ^{130}S, but no ions representing the fragment containing residues 74–94 (which contains five phosphorylation sites) are observed in either positive or negative mode. The remaining phosphorylation site, ^{130}S, is located in the 121–134 tryptic fragment; this and the 119–134 fragment (due to a missed cleavage at ^{120}K) are present with reasonable intensity in the mass spectrum as doubly protonated species at *m/z* 830.9 and *m/z* 976.5, respectively (Figure 9a). When the ions are irradiated for 20 ms (Figure 9b), the intensities of the phosphorylated ion peaks diminish due to the dissociation of the ions. The other ions in the spectrum that represent unphosphorylated species remain unaffected, demonstrating that ESI-IRMPD-MS can be used to selectively dissociate phosphorylated species in a complex mixture, allowing quick screening for phosphorylated components in any mixture, particularly tryptic digests of phosphorylated proteins.

Conclusions

IRMPD in a quadrupole ion trap has been shown to allow for both increased peptide sequence coverage over the more conventional CAD technique as well as the selective dissociation of phosphorylated peptides in complex mixtures. Alleviation of the performance-limiting low-*m/z* cutoff associated with CAD along with the production of higher order fragments results in a larger degree of sequence information for IRMPD than CAD for both phosphorylated and unphosphorylated peptides. In addition, because of the nonresonant nature of IRMPD, dead-end fragmentation pathways that are sometimes problematic for resonant activation techniques are avoided and, in the cases presented here, more sequence coverage was obtained with upon IRMPD than with two sequential CAD events (MS^3) for a pair of phosphorylated peptides. The results illustrating selective dissociation of phosphorylated peptides in complex mixtures demonstrate the potential utility of

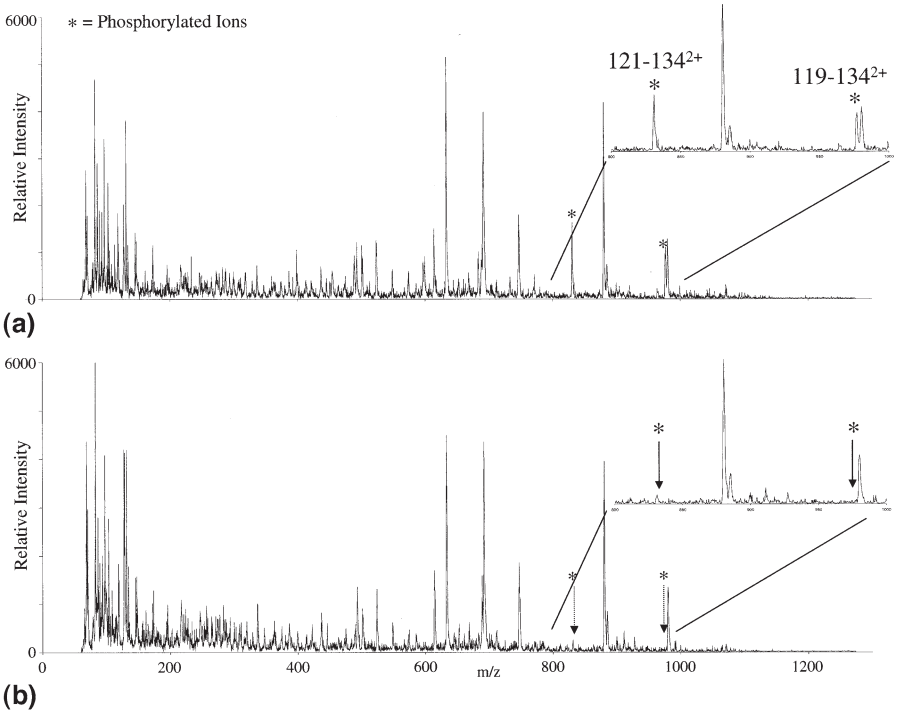

Figure 9. IRMPD mass spectra of α-casein tryptic digest (**a**) t = 0 ms, (**b**) t = 20 ms (45 watts).

IRMPD in a quadrupole ion trap to assist in the determination of sites of phosphorylation in larger, more biologically active proteins.

Acknowledgments

The authors gratefully acknowledge funding from the Welch Foundation (F1155) and the National Science Foundation (CHE-0315337).

References

1. Sun, H.; Tonks, N. K. The Coordinated Action of Protein-Tyrosine Phosphatases and Kinases in Cell Signaling. *Trends Biochem. Sci.* **1994,** *19*, 480–485.
2. Faux, M. C.; Scott, J. D. More on Target with Protein Phosphorylation: Conferring Specificity by Location. *Trends Biochem. Sci.* **1996,** *21*, 312–315.
3. Krebs, E. G. The Growth of Research on Protein-Phosphorylation. *Trends Biochem. Sci.* **1994,** *19*, 439–439.
4. Hunter, T. Protein-Kinases and Phosphatases—The Yin and Yang of Protein-Phosphorylation and Signaling. *Cell* **1995,** *80*, 225–236.
5. Posada, J.; Cooper, J. A. Molecular Signal Integration—Interplay Between Serine, Threonine, and Tyrosine Phosphorylation. *Mol. Biol. Cell* **1992,** *3*, 583–592.
6. Biemann, K. Contributions of Mass Spectrometry to Peptide and Protein Structure. *Biomed. Environ. Mass* **1988,** *16*, 99–111.
7. Carr, S. A.; Hemling, M. E.; Bean, M. F.; Roberts, G. D. Integration of Mass Spectrometry in Analytical Biotechnology. *Anal. Chem.* **1991,** *63*, 2802–2824.
8. Cohen, P.; Gibson, B. W.; Holmes, C. F. B. Analysis of the in Vivo Phosphorylation States of Proteins by Fast-Atom-Bombardment Mass Spectrometry and Other Techniques. *Methods Enzymol.* **1991,** *201*, 153–168.
9. Huddleston, M. J.; Annan, R. S.; Bean, M. F.; Carr, S. A. Selective Detection of Phosphopeptides in Complex-Mixtures by Electrospray Liquid Chromatography MassSpectrometry. *J. Am. Soc. Mass Spectrom.* **1993,** *4*, 710–717.
10. Affolter, M.; Watts, J. D.; Krebs, D. L.; Aebersold, R. Evaluation of 2-Dimensional Phosphopeptide Maps by Electrospray Ionization Mass Spectrometry of Recovered Peptides. *Anal. Biochem.* **1994,** *223*, 74–81.
11. Burlingame, A. L.; Boyd, R. K.; Gaskell, S. J. Mass Spectrometry. *Anal. Chem.* **1994,** *66*, R634–R683.
12. Hunter, A. P.; Games, D. E. Chromatographic and Mass Spectrometric Methods for the Identification of Phosphorylation Sites in Phosphoproteins. *Rapid Commun. Mass Spectrom.* **1994,** *8*, 559–570.
13. Resing, K. A.; Johnson, R. S.; Walsh, K. A. Mass-Spectrometric Analysis of 21 Phosphorylation Sites in the Internal Repeat of Rat Profilaggrin, Precursor of an Intermediate Filament-Associated Protein. *Biochemistry* **1995,** *34*, 9477–9487.
14. Carr, S. A.; Huddleston, M. J.; Annan, R. S. Selective Detection and Sequencing of Phosphopeptides at the Femtomole Level by Mass Spectrometry. *Anal. Biochem.* **1996,** *239*, 180–192.
15. Busman, M.; Schey, K. L.; Oatis, J. E.; Knapp, D. R. Identification of Phosphorylation Sites in Phosphopeptides by Positive and Negative Mode Electrospray Ionization Tandem Mass Spectrometry. *J. Am. Soc. Mass Spectrom.* **1996,** *7*, 243–249.
16. Ladner, R. D.; Carr, S. A.; Huddleston, M. J.; McNulty, D. E.; Caradonna, S. J. Identification of a Consensus Cyclin-Dependent Kinase Phosphorylation Site Unique to the Nuclear Form of Human Deoxyuridine Triphosphate Nucleotidohydrolase. *J. Biol. Chem.* **1996,** *271*, 7752–7757.
17. Annan, R. S.; Carr, S. A. Phosphopeptide Analysis by Matrix-Assisted Laser Desorption Time-of-Flight Mass Spectrometry. *Anal. Chem.* **1996,** *68*, 3413–3421.
18. Qin, J.; Chait, B. T. Identification and Characterization of Posttranslational Modifications of Proteins by MALDI Ion Trap Mass Spectrometry. *Anal. Chem.* **1997,** *69*, 4002–4009.

19. DeGnore, J. P.; Qin, J. Fragmentation of Phosphopeptides in an Ion Trap Mass Spectrometer. *J. Am. Soc. Mass Spectrom.* **1998,** *9*, 1175–1188.
20. Neubauer, G.; Mann, M. Mapping of Phosphorylation Sites of Gel-Isolated Proteins by Nanoelectrospray Tandem Mass Spectrometry: Potentials and Limitations. *Anal. Chem.* **1999,** *71*, 235–242.
21. Stensballe, A.; Jensen, O. N.; Olsen, J. V.; Haselmann, K. F.; Zubarev, R. A. Electron Capture Dissociation of Singly and Multiply Phosphorylated Peptides. *Rapid Commun. Mass Spectrom.* **2000,** *14*, 1793–1800.
22. Flora, J. W.; Muddiman, D. C. Selective, Sensitive, and Rapid Phosphopeptide Identification in Enzymatic Digests Using ESI-FTICR-MS with Infrared Multiphoton Dissociation. *Anal. Chem.* **2001,** *73*, 3305–3311.
23. Schlosser, A.; Pipkorn, R.; Bossemeyer, D.; Lehmann, W. D. Analysis of Protein Phosphorylation by a Combination of Elastase Digestion and Neutral Loss Tandem Mass Spectrometry. *Anal. Chem.* **2001,** *73*, 170–176.
24. Shi, S. D. H.; Hemling, M. E.; Carr, S. A.; Horn, D. M.; Lindh, I.; McLafferty, F. W. Phosphopeptide/Phosphoprotein Mapping by Electron Capture Dissociation Mass Spectrometry. *Anal. Chem.* **2001,** *73*, 19–22.
25. Flora, J. W.; Muddiman, D. C. Gas-Phase Ion Unimolecular Dissociation for Rapid Phosphopeptide Mapping by IRMPD in a Penning Ion Trap: An Energetically Favored Process. *J. Am. Chem. Soc.* **2002,** *124*, 6546–6547.
26. Wind, M.; Kelm, O.; Nigg, E. A.; Lehmann, W. D. Identification of Phosphorylation Sites in the Polo-Like Kinases Plx1 and PIk1 by a Novel Strategy Based on Element and Electrospray High Resolution Mass Spectrometry. *Proteomics* **2002,** *2*, 1516–1523.
27. Chalmers, M. J.; Quinn, J. P.; Blakney, G. T.; Emmett, M. R.; Mischak, H.; Gaskell, S. J.; Marshall, A. G. Liquid Chromatography-Fourier Transform Ion Cyclotron Resonance Mass Spectrometric Characterization of Protein Kinase C Phosphorylation. *J. Proteome Res.* **2003,** *2*, 373–382.
28. Flora, J. W.; Muddiman, D. C. Determination of the Relative Energies of Activation for the Dissociation of Aromatic Versus Aliphatic Phosphopeptides by ESI-FTICR-MS and IRMPD. *J. Am. Soc. Mass Spectrom.* **2004,** *15*, 121–127.
29. Chalmers, M. J.; Kolch, W.; Emmett, M. R.; Marshall, A. G.; Mischak, H. Identification and Analysis of Phosphopeptides. *J. Chromatogr. B* **2004,** *803*, 111–120.
30. Chalmers, M. J.; Hakansson, K.; Johnson, R.; Smith, R.; Shen, J. W.; Emmett, M. R.; Marshall, A. G. Protein Kinase A Phosphorylation Characterized by Tandem Fourier Transform Ion Cyclotron Resonance Mass Spectrometry. *Proteomics* **2004,** *4*, 970–981.
31. Zubarev, R. A. Electron-Capture Dissociation Tandem Mass Spectrometry. *Curr. Opin. Biotech.* **2004,** *15*, 12–16.
32. Zubarev, R. A.; Kelleher, N. L.; McLafferty, F. W. Electron Capture Dissociation of Multiply Charged Protein Cations. A Nonergodic Pprocess. *J. Am. Chem. Soc.* **1998,** *120*, 3265–3266.
33. Kelleher, R. L.; Zubarev, R. A.; Bush, K.; Furie, B.; Furie, B. C.; McLafferty, F. W.; Walsh, C. T. Localization of Labile Posttranslational Modifications by Electron Capture Dissociation: The Case of γ-Carboxyglutamic Acid. *Anal. Chem.* **1999,** *71*, 4250–4253.
34. Horn, D. M.; Ge, Y.; McLafferty, F. W. Activated Ion Electron Capture Dissociation for Mass Spectral Sequencing of Larger (42 kDa) Proteins. *Anal. Chem.* **2000,** *72*, 4778–4784.
35. Hakansson, K.; Cooper, H. J.; Emmett, M. R.; Costello, C. E.; Marshall, A. G.; Nilsson, C. L. Electron Capture Dissociation and Infrared Multiphoton Dissociation MS/MS of an N-Glycosylated Tryptic Peptide to Yield Complementary Sequence Information. *Anal. Chem.* **2001,** *73*, 4530–4536.
36. McLafferty, F. W.; Horn, D. M.; Breuker, K.; Ge, Y.; Lewis, M. A.; Cerda, B.; Zubarev, R. A.; Carpenter, B. K. Electron Capture Dissociation of Gaseous Multiply Charged Ions by Fourier-Transform Ion Cyclotron Resonance. *J. Am. Soc. Mass Spectrom.* **2001,** *12*, 245–249.
37. Hakansson, K.; Emmett, M. R.; Hendrickson, C. L.; Marshall, A. G. High-Sensitivity Electron Capture Dissociation Tandem FTICR Mass Spectrometry of Microelectrosprayed Peptides. *Anal. Chem.* **2001,** *73*, 3605–3610.
38. Syka, J. E. P.; Coon, J. J.; Schroeder, M. J.; Shabanowitz, J.; Hunt, D. F. Peptide and Protein Sequence Analysis by Electron Transfer Dissociation Mass Spectrometry; *PNAS-USA*; 2004, pp 9528–9533.
39. Little, D. P.; Speir, J. P.; Senko, M. W.; O'Connor, P. B.; McLafferty, F. W. Infrared Multiphoton Dissociation of Large Multiply-Charged Ions for Biomolecule Sequencing. *Anal. Chem.* **1994,** *66*, 2809–2815.
40. Little, D. P.; Aaserud, D. J.; Valaskovic, G. A.; McLafferty, F. W. Sequence Information from 42-108-mer DNAs (Complete for a 50-mer) by Tandem Mass Spectrometry. *J. Am. Chem. Soc.* **1996,** *118*, 9352–9359.
41. Shi, S. D. H.; Hendrickson, C. L.; Marshall, A. G.; Siegel, M. M.; Kong, F. M.; Carter, G. T. Structural Validation of Saccharomicins by High Resolution and High Mass Accuracy Fourier Transform Ion Cyclotron Resonance Mass Spectrometry and Infrared Multiphoton Dissociation Tandem Mass Spectrometry. *J. Am. Soc. Mass Spectrom.* **1999,** *10*, 1285–1290.
42. Li, W. Q.; Hendrickson, C. L.; Emmett, M. R.; Marshall, A. G. Identification of Intact Proteins in Mixtures by Alternated Capillary Liquid Chromatography Electrospray Ionization and LC ESI Infrared Multiphoton Dissociation Fourier Transform Ion Cyclotron Resonance Mass Spectrometry. *Anal. Chem.* **1999,** *71*, 4397–4402.
43. Hofstadler, S. A.; Sannes-Lowery, K. A.; Griffey, R. H. Infrared Multiphoton Dissociation in an External Ion Reservoir. *Anal. Chem.* **1999,** *71*, 2067–2070.
44. Hakansson, K.; Hudgins, R. R.; Marshall, A. G. Electron Capture Dissociation and Infrared Multiphoton Dissociation of Oligodeoxynucleotide Dications. *J. Am. Soc. Mass Spectrom.* **2003,** *14*, 23–41.
45. Drader, J. J.; Hannis, J. C.; Hofstadler, S. A. Infrared Multiphoton Dissociation with a Hollow Fiber Waveguide. *Anal. Chem.* **2003,** *75*, 3669–3674.
46. Hofstadler, S. A.; Drader, J. J.; Gaus, H.; Hannis, J. C.; Sannes-Lowery, K. A. Alternative Approaches to Infrared Multiphoton Dissociation in an External Ion Reservoir. *J. Am. Soc. Mass Spectrom.* **2003,** *14*, 1413–1423.
47. Xie, Y. M.; Lebrilla, C. B. Infrared Multiphoton Dissociation of Alkali Metal-Coordinated Oligosaccharides. *Anal. Chem.* **2003,** *75*, 1590–1598.
48. Stephenson, J. L.; Booth, M. M.; Shalosky, J. A.; Eyler, J. R.; Yost, R. A. Infrared Multiple-Photon Dissociation in the Quadrupole Ion-Trap via a Multipass Optical Arrangement. *J. Am. Soc. Mass Spectrom.* **1994,** *5*, 886–893.
49. Colorado, A.; Shen, J. X. X.; Vartanian, V. H.; Brodbelt, J. Use of Infrared Multiphoton Photodissociation with SWIFT for Electrospray Ionization and Laser Desorption Applications in a Quadrupole Ion Trap Mass Spectrometer. *Anal. Chem.* **1996,** *68*, 4033–4043.
50. Stephenson, J. L.; Booth, M. M.; Boue, S. M.; Eyler, J. R.; Yost, R. A. Analysis of Biomolecules Using Electrospray Ionization Ion-Trap Mass Spectrometry and Laser Photodissociation. *ACS Symposium Series* **1996,** *619*, 512–564.
51. Goolsby, B. J.; Brodbelt, J. S. Characterization of β-Lactams by Photodissociation and Collision-Activated Dissociation in a Quadrupole Ion Trap. *J. Mass Spectrom.* **1998,** *33*, 705–712.

52. Vartanian, V. H.; Goolsby, B.; Brodbelt, J. S. Identification of Tetracycline Antibiotics by Electrospray Ionization in a Quadrupole Ion Trap. *J. Am. Soc. Mass Spectrom.* **1998,** *9*, 1089–1098.
53. Goolsby, B. J.; Brodbelt, J. S. Analysis of Protonated and Alkali Metal Cationized Aminoglycoside Antibiotics by Collision-Activated Dissociation and Infrared Multi-Photon Dissociation in the Quadrupole Ion Trap. *J. Mass Spectrom.* **2000,** *35*, 1011–1024.
54. Shen, J.; Brodbelt, J. S. Characterization of Ionophore-Metal Complexes by Infrared Multiphoton Photodissociation and Collision-Activated Dissociation in a Quadrupole Ion Trap Mass Spectrometer. *Analyst* **2000,** *125*, 641–650.
55. Payne, A. H.; Glish, G. L. Thermally Assisted Infrared Multiphoton Photodissociation in a Quadrupole Ion Trap. *Anal. Chem.* **2001,** *73*, 3542–3548.
56. Goolsby, B. J.; Brodbelt, J. S. Tandem Infrared Multiphoton Dissociation and Collisionally Activated Dissociation Techniques in a Quadrupole Ion Trap. *Anal. Chem.* **2001,** *73*, 1270–1276.
57. Crowe, M. C.; Brodbelt, J. S.; Goolsby, B. J.; Hergenrother, P. Characterization of Erythromycin Analogs by Collisional Activated Dissociation and Infrared Multiphoton Dissociation in a Quadrupole Ion Trap. *J. Am. Soc. Mass Spectrom.* **2002,** *13*, 630–649.
58. Gabryelski, W.; Li, L. Photoinduced Dissociation of Electrospray-Generated Ions in an Ion Trap/Time-of-Flight Mass Spectrometer Using a Pulsed CO2 Laser. *Rapid Commun. Mass Spectrom.* **2002,** *16*, 1805–1811.
59. Hashimoto, Y.; Hasegawa, H.; Yoshinari, K.; Waki, I. Collision-Activated Infrared Multiphoton Dissociation in a Quadrupole Ion Trap Mass Spectrometer. *Anal. Chem.* **2003,** *75*, 420–425.
60. Keller, K. M.; Brodbelt, J. S. Collisionally Activated Dissociation and Infrared Multiphoton Dissociation of Oligonucleotides in a Quadrupole Ion Trap. *Anal. Biochem.* **2004,** *326*, 200–210.
61. Silverstein, R. M.; Bassler, G. C.; Morrill, T. C. In *Spectrometric Identification of Organic Compounds*; Wiley: New York, 1981; p 170.
62. Vanberkel, G. J.; Glish, G. L.; Mcluckey, S. A. Electrospray Ionization Combined with Ion Trap Mass Spectrometry. *Anal. Chem.* **1990,** *62*, 1284–1295.